The Discovery of III-V Oxidation, Device Progress, and Application to Vertical-Cavity Surface-Emitting Lasers

J.M. Dallesasse

Department of Electrical and Computer Engineering, University of Illinois at Urbana-Champaign, Urbana, IL, 61801 USA
jdallesa@illinois.edu, (217) 333-8416

Keywords: III-V oxidation, VCSELs, semiconductor lasers, III-V materials, device fabrication, optical communications

Abstract

The discovery of III-V oxidation and subsequent application of oxide technology to the fabrication of semiconductor lasers are reviewed. Work on lateral oxidation and the application of laterally oxidized layers to form optically and electrically confining apertures is discussed, as well as the commercially-significant use of lateral oxides in vertical-cavity surface-emitting lasers.

INTRODUCTION

Since the discovery of III-V Oxidation by Dallesasse and Holonyak in 1989, significant progress has been made both technically and commercially on the use of oxides in compound semiconductor devices. The process-induced modification of refractive index and conductivity allows control of the two carriers of information in opto-electronic systems, the photon and the electron, enabling wide-ranging device applications. Of particular note has been the use of oxidation for the fabrication of high-speed Vertical-Cavity Surface-Emitting Lasers (VCSELs). The discovery of III-V Oxidation and key technical milestones in the fabrication of photonic and electronic devices that use oxidation are reviewed, with an emphasis on VCSEL progress.

THE DISCOVERY OF III-V OXIDATION

The discovery of III-V Oxidation in 1989 by Dallesasse and Holonyak began with the examination of material degradation in high-composition $Al_xGa_{1-x}As$.[1] Samples containing AlAs layers buried within a multilayer epitaxial structure were observed to erode over time due to exposure to room-ambient humidity and temperature. For a specific set of samples, this erosion was tracked and documented over a multi-year period.

In the further study of this degradation process, oxidation was discovered. Specifically, an AlAs layer was directly exposed to a steam ambient, and a uniform oxide was observed across the surface of the wafer.[2] This oxide was found to be mechanically stable against abrasion using q-tip and rubber eraser tests, well adhered to the wafer surface using a "Scotch Tape Test," and resistant to typical chemicals used in compound semiconductor wafer processing. In Figure 1, we show a recent (February, 2012) photograph that illustrates the uniformity and stability of the oxide process (right 50 mm diameter wafer) compared to a piece of a wafer grown in 1978 containing high-composition $Al_xGa_{1-x}As$ layers that have hydrolyzed (left).

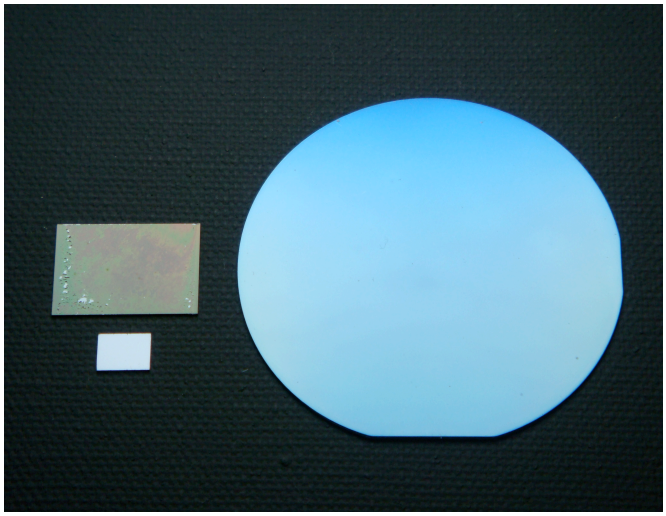

Figure 1. Photograph of three $Al_xGa_{1-x}As$-GaAs samples showing the stability of oxidation (right), instability of high-composition $Al_xGa_{1-x}As$ (left), and bare, polished GaAs (lower left).

The small wafer piece sitting below the degraded sample shows the reverse side of the hydrolyzed wafer, a polished GaAs surface upon which no material was grown, illustrating the stability of the base substrate. An important point to note is that the oxidized wafer on the right was oxidized in August of 1991, and shows no signs of deterioration or change after 21 years. While the significant body of data showing the reliability of oxide-confined VCSELs can be pointed to when addressing the question of the overall robustness of the process,[3] this wafer is a clear visual indication of the stability of materials formed through III-V Oxidation.

In addition to surface oxidation, early oxidation experiments also included the exposure of AlAs-GaAs superlattice edges to steam environments. Lateral oxidation was demonstrated by this work, as well as the fact that the rate of lateral oxidation has a dependence on the thickness of the layers being oxidized.[2] An optical photomicrograph revealing lateral oxidation is shown in Figure 2. Zinc diffusion had been performed in the field region forming,

through layer intermixing, material of average composition ~$Al_{0.8}Ga_{0.2}As$ surrounding an intact SL "dot." In this sample, the substrate is removed prior to oxidation and white light transmission through the sample is shown in the photomicrograph. For the regions where the layers of the SL are not exposed at a cleaved edge lateral oxidation is not observed – the "dot" remains red (dark grey). In the case where the SL layers can be accessed at the edge with a cleave passing through the "dot" containing SL layers, as highlighted by the downward pointing arrow at the wafer edge in the figure, edge oxidation proceeds and the dot begins to be converted into an oxide. The transparency of the oxide is also evident. A significant difference in the rate of lateral oxidation is observed between material having thicker AlAs layers versus thinner AlAs layers.

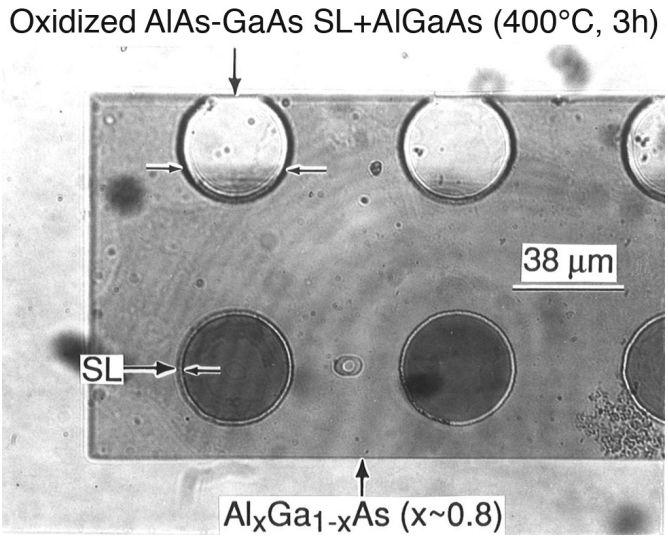

Figure 2. Optical photomicrograph (transmission) showing lateral (edge) oxidation in an AlAs-GaAs superlattice sample. Reprinted with permission from Appl. Phys. Lett. **57**, 2844 (1990). Copyright 1990 American Institute of Physics.

The capability to create both surface and subterranean oxide layers creates a vast number of possibilities for use in both discrete devices and photonic integration – a fact that was immediately recognized.

Device Applications

The first devices fabricated using the oxidation process were edge-emitting quantum well heterostructure lasers.[4] Results from Illinois on multi-stripe laser arrays rapidly followed the work on individual emitters.[5] This work highlighted the fact that the oxide can be used to provide both current and optical confinement. For multi-stripe laser arrays, the coupling between adjacent laser stripes can be controlled by changing oxidation depth and as a consequence the effective index step between the electrically pumped and oxidized regions. A scanning electron microscope (SEM) photomicrograph of a multi-stripe laser array where surface oxidation is used to define the emitting regions across a 200 μm total aperture width is presented in Figure 3. This laser, designed for diode-pumped solid-state laser applications, operates to optical output powers in excess of 4 W before experiencing roll-over.[6]

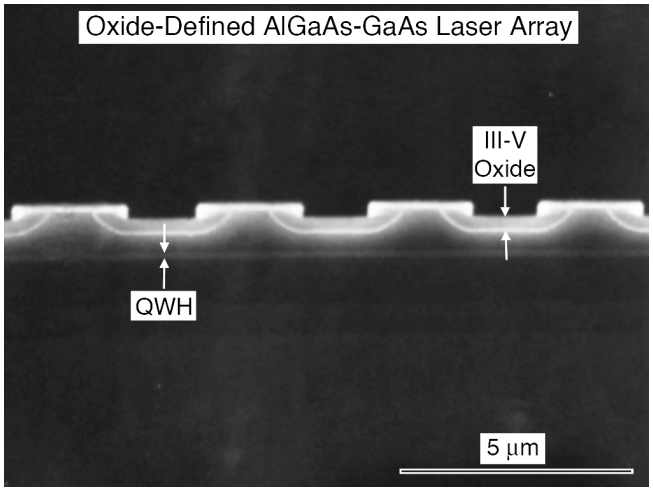

Figure 3. SEM photomicrograph of a multi-stripe edge-emitting laser array for diode-pumped solid-state laser applications. Reprinted with permission from J. Appl. Phys. **113**, 051101 (2013). Copyright 2013 American Institute of Physics.

A significant body of work has followed these initial demonstrations. Among the more significant contributions has been the use of oxidation to form lateral oxide apertures in edge-emitting lasers,[7] the application of oxidation to aluminum-bearing material systems other than $Al_xGa_{1-x}As$, [8,9] the use of oxidation to improve the reliability of high-brightness LEDs,[10] work on III-V Oxide FETs,[11,12] and the use of oxide apertures in the Holonyak-Feng transistor laser.[13] The most significant commercial success has been in the area of VCSELs, where the ability to provide both optical and current confinement significantly enhances laser performance.[14]

Systems for III-V Oxidation

The design of furnaces for wet oxidation has evolved as the understanding of the process has grown. Early work was conducted in very simple open-tube systems using quartz tubes with ground-glass end cap seals. For loading, samples were placed on flat quartz boats and loaded into open furnaces with push rods. No care was taken to control residual oxygen. Water vapor was provided by bubbling nitrogen through water-filled gas wash bottles wrapped with heat tape to maintain a water temperature of ~95°C. These were connected to the furnace with Teflon tubing.

The best system designs today are designed to provide more optimal conditions for sample loading, better control of residual oxygen levels, and improved gas handling for water vapor, push gas (nitrogen), and other gasses such as oxygen which may be desired in controlled amounts for specific materials. In some cases, baffles are used to improve gas flow uniformity and uniformity of oxidation rates across the sample. The furnace exhaust is typically passed over a

condenser to trap oxidation byproducts (arsenic oxides), and passes through a bubbler to minimize uncontrolled residual oxygen levels by preventing backstreaming from the exhaust into the system under low flow conditions. These improvements in furnace design have led to improved process consistency and better surface morphology. The chemical characteristics of the oxidized layer may also be affected by factors related to furnace design such as residual oxygen, even in small amounts. The process is more complex than silicon oxidation, as one would expect due to the number of species involved in the reaction (Al, Ga, As, etc.). There are inconsistencies in the literature examining III-V oxidation rates and mechanisms, likely a consequence of differences in furnace design and residual oxygen levels.

VCSEL Progress

It has long been known that the magnitude of the gain in a direct-gap semiconductor allows the possibility of both small-volume in-plane (edge-emitting) and perpendicular-to-plane (surface-emitting) lasers. Early demonstrations of perpendicular-to-plane laser operation were made in e-beam [15] and optically pumped micro-volume lasers.[16] Current-injected devices were also demonstrated in InSb.[17] The first device to resemble a modern VCSEL appears in a Scifres, et al. patent filed in 1975.[18] This device uses a vertical structure consisting of alternating $Al_xGa_{1-x}As$-GaAs layers to form a Bragg reflector, but contemplates a p-n junction geometry perpendicular to the Bragg planes with each GaAs mirror element providing gain. Experimental work on p-n junction surface-emitting lasers with a vertical cavity but metal mirrors was initiated by Iga [19] and moved forward by other groups. An important advance in VCSEL technology, made in 1994 at The University of Texas at Austin by the Deppe group,[12] is the application of lateral oxidation to form apertures for optical and carrier confinement. Deppe, who had been studying air voids to control VCSEL optical modes, realized that oxidized material would be an ideal alternative with better reproducibility. Since the distance of lateral oxidation can be controlled through time and temperature, oxidation provides a scalable, manufacturable method for forming small-diameter lasers from larger diameter mesas. Work on oxide-aperture VCSEL in the ~850nm wavelength range has been advanced by a number of groups, eventually leading to commercial devices. Progress has also been made on oxide-confined VCSELs operating in the metro and telecom wavelength ranges of 1310 and 1550 nm, but commercial success here has been more limited. A cross-sectional diagram of a typical VCSEL structure is shown in Figure 4. Several features typical for commercial devices are shown in this figure, though not all of these may be present in any given device. The unifying element is the oxide aperture. Small-diameter apertures are important electrically for the realization of high-speed device operation, enabling applications such as 10 Gigabit Ethernet and high-speed links in the data center. Optically, applications such as computer mice (position sensors) and high-end printing require the control of the characteristics of the spatial modes of the device made possible using the large index change effected by oxidation.

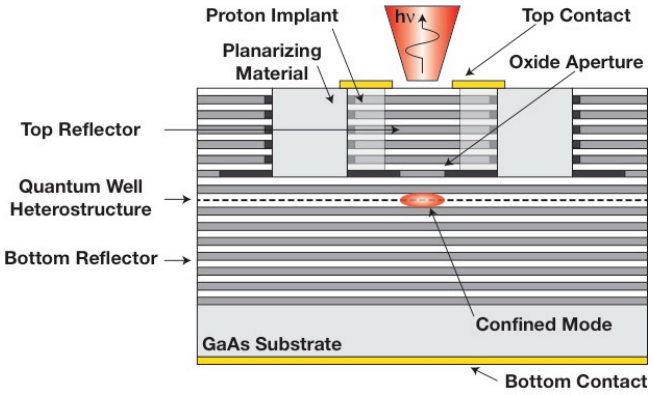

Figure 4. Diagram showing the typical cross section of an oxide-confined VCSEL.

Work on oxide-confined VCSELs continues to advance as the need for higher speed data links for data center applications becomes more pressing. A representative eye diagram for a high-speed VCSEL produced by Sumitomo Electric Device Innovations USA is presented in Figure 5. This device is being operated at a data rate of 25 Gbps and a temperature of 85°C.

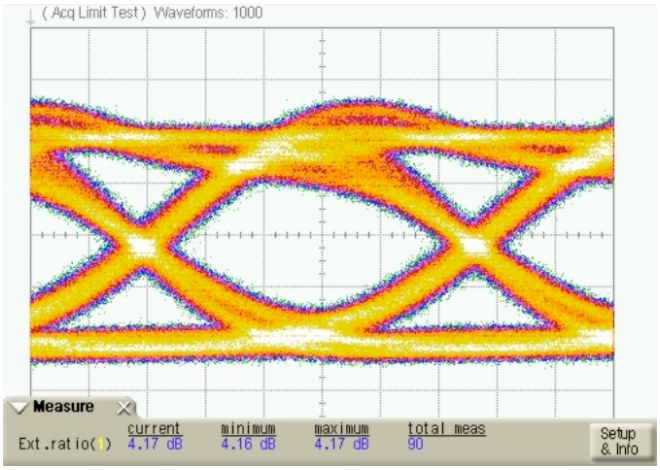

Figure 5. Optical eye diagram (85°C) for a Sumitomo Electric Device Innovations (SEDU) VCSEL being operated at 25 Gbps using a PRBS31 bit sequence. The time scale is 7 picoseconds per major division.

The PRBS31 signal is delivered through a RF probe, with DC bias provided through a bias tee. No pre-emphasis is added to the signal. The eye diagrams are of good quality, clearly showing promise for the inevitable migration of link speeds for short-haul applications from 10 Gbps to 25 Gbps per channel. Other groups working on microcavity devices have continued to push toward smaller aperture size to further improve the maximum 3 dB bandwidth. For example, Tan, et al.[20] have shown microcavity VCSELs with a 3 μm oxide aperture having a 3 dB bandwidth of

greater than 19 GHz. Work continues to further improve device speed and reliability.

CONCLUSIONS

Oxidation of Al-bearing III-V compound semiconductor materials has proven to be an important technology for the fabrication of optoelectronic devices, and with further work may be useful for electronic devices as well. The process-induced change in material properties allows for optical mode control, control of current injection, and control of channel conductivity in field-effect devices. The commercial success of the oxide-confined VCSEL has established that oxide-based devices are both reliable and manufacturable, making oxidation an important processing technique for compound semiconductor devices.

ACKNOWLEDGEMENTS

The author would like to thank Nick Holonyak, Jr., for ongoing encouragement and inspiration. Additionally, I would like to thank Milton Feng for helpful discussions. Finally, I would like to thank and acknowledge Chris Wiggins, Ken Jackson, Nelson Li, and Chuan Xie at Sumitomo Electric Device Innovations USA for providing eye diagrams for their 25 Gbps-capable VCSELs.

REFERENCES

[1] J.M. Dallesasse, P. Gavrilovic, N. Holonyak, Jr., R.W. Kaliski, D.W. Nam, and E.J. Vesely, "Stability of AlAs in $Al_xGa_{1-x}As$-AlAs-GaAs quantum well heterostructures," Appl. Phys. Lett. **56** (24), 2436 (1990).

[2] J. M. Dallesasse, N. Holonyak, Jr., A. R. Sugg, T. A. Richard, and N. El-Zein, "Hydrolyzation Oxidation of $Al_xGa_{1-x}As$-AlAs-GaAs Quantum Well Heterostructures and Superlattices," Appl. Phys. Lett. **57**, 2844 (1990).

[3] N. Li, C. Xie, W. Lou, C.J. Helms, L. Wang, C. Liu, Q. Sun, S. Huang, C. Lei, K.P. Jackson, R.F. Carson, "Emcore's 1Gb/s to 25 Gb/s VCSELs," Proc. SPIE 8276, Vertical-Cavity Surface-Emitting Lasers XVI, 827603 (Feb. 9, 2012).

[4] J. M. Dallesasse and N. Holonyak, "Native-Oxide Stripe-Geometry $Al_xGa_{1-x}As$-GaAs Quantum Well Heterostructure Lasers," Jr., Appl. Phys. Lett. **58**, 394 (1991).

[5] J. M. Dallesasse, N. Holonyak, Jr., D. C. Hall, N. El-Zein, A. R. Sugg, S. C. Smith, and R. D. Burnham, "Native-Oxide Defined Coupled-Stripe $Al_xGa_{1-x}As$-GaAs Quantum-Well Heterostructure Lasers," Appl. Phys. Lett. **58**, 834 (1991).

[6] J.M. Dallesasse and N. Holonyak, Jr., "Oxidation of Al-bearing III-V materials: A review of key progress," J. Appl. Phys. **113**, 051101 (2013).

[7] S.A. Maranowski, A.R. Sugg, E.I. Chen, and N. Holonyak, Jr., "Native oxide top- and bottom-confined narrow stripe p-n $Al_yGa_{1-y}As$-GaAs-$In_xGa_{1-x}As$ quantum well heterostructure laser," Appl. Phys. Let. **63** (12), 1660 (1993).

[8] F.A. Kish, S.J. Caracci, N. Holonyak, Jr., J.M. Dallesasse, A.R. Sugg, R.M. Fletcher, C.P. Kuo, T.D. Osentowski, and M.D. Craford, "Native-oxide stripe-geometry $In_{0.5}(Al_xGa_{1-x})_{0.5}P$-$In_{0.5}Ga_{0.5}P$ heterostructure laser diodes," Appl. Phys. Lett. **59** (3), 354 (1991).

[9] M.R. Krames, N. Holonyak, Jr., J.E. Epler, and H.P. Schweizer, "Buried-oxide ridge-waveguide InAlAs-InP-InGaAsP (l~1.3 mm) quantum well heterostructure laser diodes," Appl. Phys. Lett. **64** (21), 2821 (1994).

[10] T.A. Richard, N. Holonyak, Jr., F.A. Kish, M.R. Keever, and C. Lei, "Postfabrication native-oxide improvement of the reliability of visible-spectrum AlGaAs-In(AlGa)P p-n heterostructure diodes," Appl. Phys. Lett. **66** (22), 2972 (1995).

[11] E.I. Chen, N. Holonyak, Jr., and S.A. Maranowski, "$Al_xGa_{1-x}As$-GaAs metal-oxide semiconductor field effect transistors formed by lateral water vapor oxidation of AlAs," Appl. Phys. Lett. **66** (20), 2688 (1995).

[12] X. Li, Y. Cao, D.C. Hall, P. Fay, B. Han, A. Wibowo, and N. Pan, "GaAs MOSFET Using InAlP Native Oxide as Gate Dielectric," IEEE Electron Device Lett. **25** (12), 772 (2004).

[13] G. Walter, N. Holonyak, Jr., M. Feng, and R. Chan, "Laser operation of a heterojunction bipolar light-emitting transistor," Appl. Phys. Lett. **85** (20), 4768 (2004).

[14] D.L. Huffaker, D.G. Deppe, K. Kumar, and T.J. Rogers, "Native-oxide defined ring contact for low threshold vertical-cavity lasers," Appl. Phys. Lett. **65** (1), 97 (1994).

[15] N.G. Basov, O.V. Bogdankevich, and A.G. Devyatkov, "Exciting of a semiconductor quantum generator with a fast electron beam," Sov. Phys. Doklady **9**, 288 (1964).

[16] G.E. Stillman, M.D. Sirkis, J.A. Rossi, M.R. Johnson, and N. Holonyak, "Volume excitation of an ultrathin single-mode CdSe laser," Appl. Phys. Lett. **9** (7), 268 (1966).

[17] I. Melngailis, "Longitudinal injection-plasma laser of InSb," Appl. Phys. Lett. **6** (3), 59 (1965).

[18] D.R. Scifres, and R.D. Burnham, "DISTRIBUTED FEEDBACK DIODE LASER," U.S. Patent 3,983,509, Sept. 28, 1976.

[19] H. Soda, K. Iga, C. Kitahara, and Y. Suematsu, "GaInAsP/InP Surface Emitting Injection Lasers," Jpn. J. Appl. Phys. 18 (12), 2329 (1979).

[20] F. Tan, C.H. Wu, M. Feng, and N. Holonyak, Jr., "Energy efficient microcavity lasers with 20 and 40 Gb/s data transmission," Appl. Phys. Lett. 98, 191107 (2011).

ACRONYMS

VCSEL: Vertical-Cavity Surface-Emitting Laser
SL: Superlattice
SEM: Scanning Electron Microscope
LED: Light Emitting Diode
FET: Field Effect Transistor
Gbps: Gigabits per second
PRBS: Pseudo Random Binary Sequence